Towards the Production of Radiotherapy Treatment Shells on 3D printers using data derived from DICOM CT and MRI: preclinical feasibility studies.

[1] *Laycock S D,* [2] *Hulse M,* [3] *Scrase C D,* [5,6]*Tam M D,* [3]*Isherwood S,* [7]*Mortimore D B,* [3]*Emmens D,* [2]*Patman J,* [8]*Short S C,* [1,4]*Bell G D.*

[1]School of Computing Sciences, University of East Anglia, Norwich, NR4 7TJ

[2] Department of Health Studies, University Campus Suffolk , Ipswich, IP4 1QJ.

[3]Department of Clinical Oncology, Ipswich Hospital NHS Trust, Ipswich, IP4 5PD.

[4] East Anglian Experimental Radiography, Modelling and 3D printing Group, School of Science, Technology and Health, University Campus Suffolk , Ipswich, IP4 1QJ.

[5]Radiology Department, Southend University Hospital NHS Foundation Trust, Southend, SS0 0RY.

[6]Postgraduate Medical Institute, Anglia Ruskin University, Chelmsford, CM1 1SQ

[7] Newbourne Solutions Ltd, Newbourne, Woodbridge, IP12 4NR, UK

[8]Leeds Institute of Cancer Studies and Pathology, University of Leeds and St James's Institute of Oncology, Leeds, LS9 7TF

Abstract

Immobilisation for patients undergoing brain or head and neck radiotherapy is achieved using perspex or thermoplastic devices that require direct moulding to patient anatomy. The mould room visit can be distressing for patients and the shells do not always fit perfectly. In addition the mould room process can be time consuming. With recent developments in 3D printing technologies comes the potential to generate a treatment shell directly from a computer model of a patient. Typically, a patient requiring radiotherapy treatment will have had a CT scan and if a computer model of a shell could be obtained directly from the CT data it would reduce patient distress, reduce visits, obtain a close fitting shell and possibly enable the patient to start their radiotherapy treatment more quickly. This paper focusses on the first stage of generating the front part of the shell and investigates the dosimetric properties of the materials to show the feasibility of 3D printer materials for the production of a radiotherapy treatment shell. The majority of the possible candidate 3D printing materials tested result in very similar attenuation of a therapeutic RT beam as the Orfit soft-drape masks currently in use in many UK radiotherapy centres. The costs involved in 3d printing are reducing and the applications to medicine are becoming more widely adopted. In this paper we show that 3D printing of bespoke radiotherapy masks is feasible and warrants further investigation.

Introduction

Typical methods for constructing radiotherapy treatment shells include high-temperature thermoplastics (e.g. cellulose acetate butyrate) moulded onto a plaster positive of the patient's face and low-temperature soft-drape thermoplastic devices that require direct moulding to the patient's face [1, 2-4]. Both of these methods involve procedures that can be distressing for patients and the resulting shells do not always fit perfectly. Sharp et al. state that the mask making process, coupled with the ongoing stress of cancer diagnosis can lead to an acute anxiety or state of panic [5]. In this paper the feasibility of using 3D printers to directly construct either a "positive" face or a treatment ("negative") shell from CT or MRI data is investigated. Techniques to construct three dimensional geometric models which can be interpreted by 3D printers are developed and the suitability of a range of 3D printer materials is determined by testing their dosimetric properties in comparison to existing immobilisation shell materials. Creating masks directly from the CT or MRI data will alleviate the need for moulding of the mask to the patients' face. Helen Bulbeck of the BrainsTrust recently conducted a survey on the impact of having a radiotherapy shell made and 50% of the respondents found the experience horrific. Additionally the Macmillan website describes the plaster process as potentially uncomfortable [6].

Previously, the authors have used techniques to utilise CT and MRI datasets for medical [7] and cultural heritage [8] applications. A recent review article [9] highlighted some of the possible clinical applications of using physical 3D models derived from CT data created by rapid prototyping. There has been work on the use of 3D surface scanning techniques in combination with 3D printing to generate radiotherapy (RT) treatment shells [10, 11], however, the authors are not aware of other published research using Digital Communications in Medicine (DICOM) data derived from either CT or MRI scans to generate such shells. Since CT and MRI technology is readily available it seems logical to investigate the potential of using this type of data to aid in the construction of anatomically accurate radiotherapy treatment shells. In light of preliminary findings [12] and an earlier study [1] methods are presented for working with both CT and MRI datasets. The suitability of a variety of 3D printer materials for use during radiotherapy treatment is also investigated and discussed.

Materials and Methods

The head and neck of a whole body CT scan was reconstructed at a slice thickness of 3.75mm and the DICOM data set was then processed using Tomomask software (www.tomomask.com) with the following stages:

1. Masking - removal of any extraneous items/features from the images which would cause problems during the automatic segmentation process (e.g. support materials or image distortions caused by metal fillings/teeth etc).
2. Segmentation - identification of the flesh/air boundary by straightforward thresholding of the pixel intensity values.
3. Binarisation - conversion of the images to black and white (white areas will subsequently be printed) where the interior of the head and neck (from the flesh boundary) is solid white and the exterior, 'air', is black. This step was performed using an automatic flood fill operation.
4. Conversion to a hollowed out "positive" head (to save on printer material) - a reduced size version of the head and neck was created by 3D erosion using a spherical structuring element of 6mm radius. A 'positive' head was then created by setting the pixels of the eroded head and neck to black.
5. Creation of a 'negative' shell - firstly, a positive is created around which the negative shell can be wrapped. The head and neck are dilated slightly (1px) to give a small tolerance for fitting. As the shell must be pulled over the head, there can be no parts of the shell which wrap behind the head. This is achieved by applying a $1 \times \infty$ pixel linear dilation directed towards the plane at the rear of the head (i.e. each white pixel is converted into a line of white pixels running towards the image lower edge). A negative shell was then created by 3D dilation of the white pixels (using a spherical structuring element) before setting the original white pixels to black.
6. Conversion to a Surface-Tessellation-Language (STL) file format prior to 3D printing - the white areas of the images, forming the positive and negative shells (created in steps 4 & 5 above), were then converted to STL files using the Tomomask 'Export to STL' feature based upon a marching cubes algorithm.

The two STL files produced (i.e. both the 'positive head and neck' and the 'negative' shell) were printed using a Z-Corps 650 printer. The full size positive head and neck was used to test the production of a soft-drape shell. A 50% of full size 'positive' head and neck was also printed to test the production of a traditional high temperature beam direction shell (BDS).

A head and neck MRI was also performed on a volunteer (co-author: M. D. Tam), using a 1.5T GE magnet (Fig 1(a)). A 3D volume scan was acquired axially using a 3D fast spoiled gradient echo (FSPGR) sequence, TR 12.2ms, TE 5.0ms, TI 450ms, with a FOV of 44x44cm, and a matrix size of 256 x 224 with 1 NEX (number of excitations). 182 images with a slice thickness of 2.0 mm and 0.55 mm slice gap were obtained with a scan time of less than 12 minutes. The DICOM data set from the MRI scan was then processed using Osirix software (www.osirix-viewer.com) using threshold segmentation, where the user controls the threshold levels for the segmentation, to convert the image into a binary dataset of black and white pixels. These were then further processed using Tomomask as above to produce a hollowed-out 'positive' of the head and neck (Fig 1(b)) and a 'negative' STL shell to fit the 'positive' head and neck of the volunteer (Fig 1(c)). The STL files were then printed at 50% size for a 3D print of the 'positive' hollowed-out head and neck model (Fig 1(d)) and at 50% size for a 3D print of the 'negative' head shell, both of which were printed out using the Z-Corps 450 3D printer. In addition, using just the face part of the 'negative' shell's STL file, a 'negative' shell was printed at full scale by Objet Printer Solutions UK Ltd using an Eden250 system with Objet's 'VeroWhitePlus' material (Fig 1(e)).
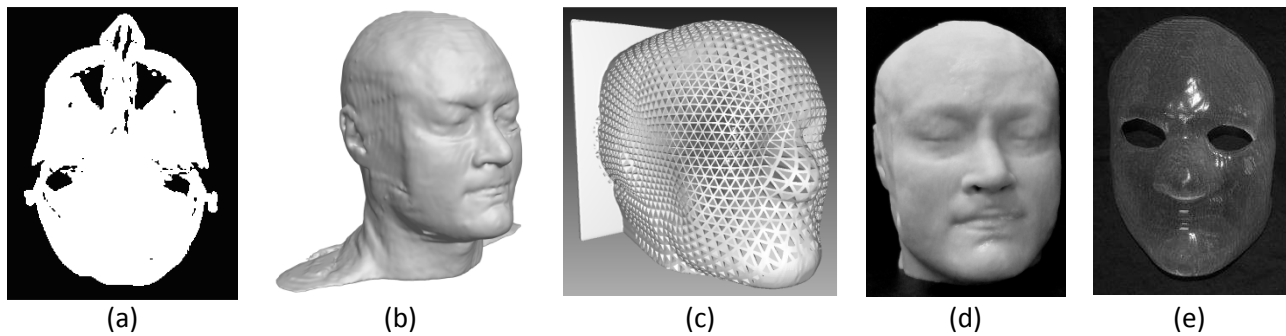
Fig 1: Constructing the masks from MRI data. (a) Image of a slice of the MRI data which has been segmented using Osirix, (b) 3D computer model of the head derived from the segmented MRI data set, (c) Edited 'negative' shell (holes were subsequently formed in the shell to demonstrate the possibility of further reducing material cost), (d) 3D print of the model of the head and (e) 3D print of an example 'negative' shell.

Dosimetric Properties of 3D Printing Materials

In our experiment we measured the change in dose produced by three materials suitable for 3D printing. These were compared with a 2.4 mm thick 'unstretched' thermoplastic 'soft drape' radiotherapy shell produced by Orfit (http://www.orfit.com/en/radiation-oncology-patient-immobilization-and-positioning/), which represents a standard material.

Measurements were made in a water equivalent material irradiated with a 10 x10 cm^2 beam of energy 6MV. The dose was measured at two points.
   (i)   5 cm deep in water using a 0.6 cm^3 Farmer chamber.
   (ii)   1 mm deep in water using a Roos chamber.
In both cases the radiation source to chamber distance was 100 cm. The dose was measured with and without the test materials placed on top of the water equivalent material. For each setup, three repeat readings were acquired with a standard deviation of less than 0.1%. For point (i), the change in dose produced by the material (ΔD_{5cm}) assesses its effect on the dose to the tumour. For point (ii), the change in the dose (ΔD_{1mm}) represents its effect on the dose to the skin.

Results

The dosimetric properties of the 3D printing materials are summarised in Fig 2. Fig 2(a) shows that all the materials produce a small decrease (up to 1%) in the dose to the tumour due to attenuation of the beam. The 2mm materials produce lower attenuation than the Orfit mask. Fig 2(b) shows that all of the materials produce an increase in skin dose between 54% to 80%. This can be minimised by using the thinner materials. The skin dose for the 2 mm materials is similar or lower than the Orfit mask.
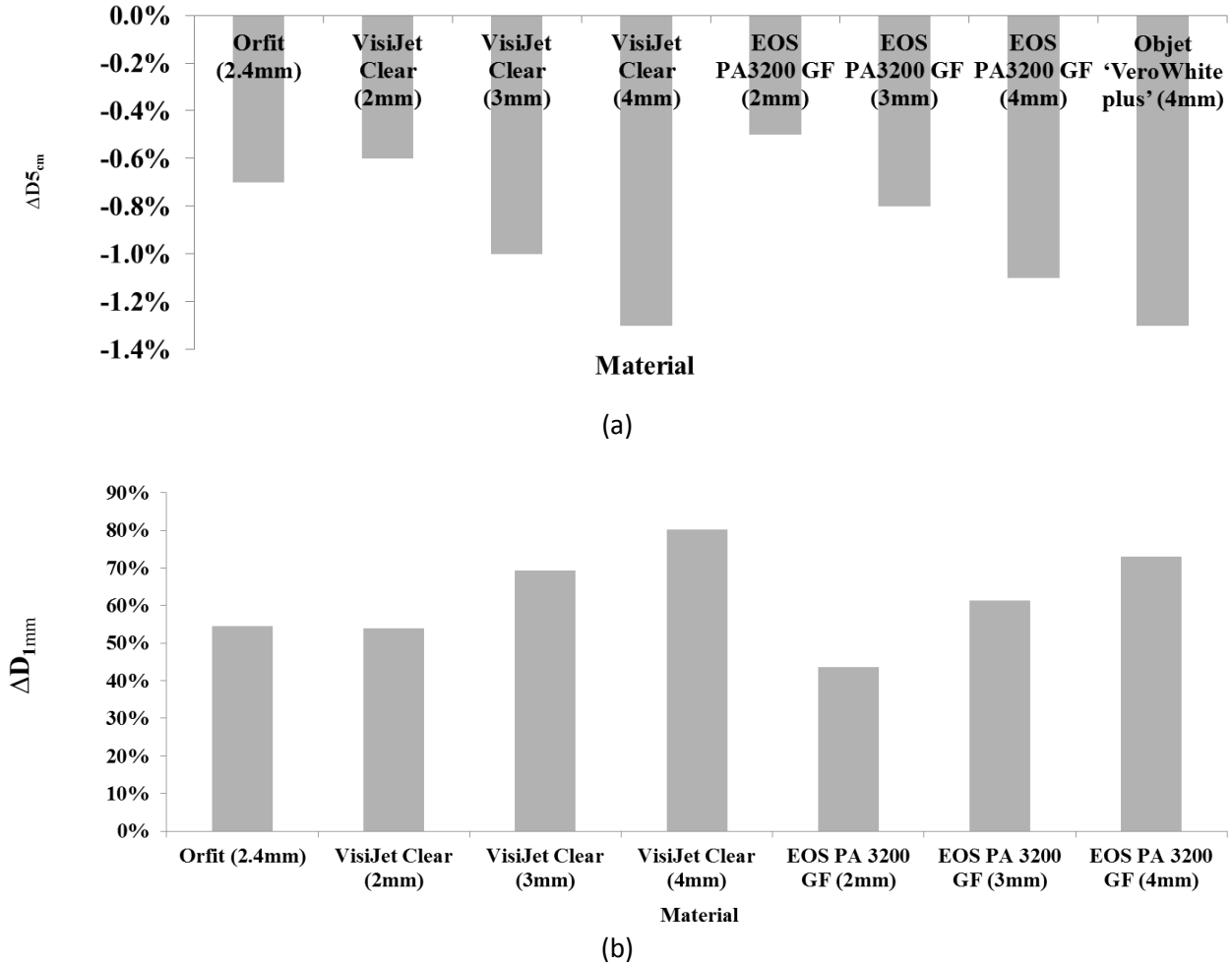

(a)

(b)

Fig 2: (a) The change in dose at 5 cm depth, ΔD_{5cm} for the Orfit thermoplastic mask in comparison to three different 3D printer materials. (b) The change in dose at 1mm depth for the Orfit thermoplastic mask in comparison to three different 3D printer materials.

Discussion

The initial stage in the process for constructing the mask is to first perform a CT scan of the patient in the intended treatment position without an immobilisation shell. This represents a change in the standard practice although can be achieved with reference to standard set up instructions as would be used in conventional mask production, provided that the patient is comfortable and stable during the CT scan. Once the CT or MRI scan has been obtained the head must be segmented from the background. There is a clear edge between the data set and surrounding air which aids the segmentation step but further evaluation to ensure this segmentation is accurate for skin is required. Furthermore, motion during the MRI sequence can blur the edges. This was seen particularly at the orbits, which can lead to artefacts causing errors up to 1mm that can be detrimental in some cases.

When constructing radiotherapy shells on a 3D printer the material used is fundamental as an ideal material should not affect the radiation dose delivered to the patient. Ideally the 3D printer material chosen should perform at least as well as the materials used in conventional methods. We found that 2mm samples of Visijet clear and EOS PA 3200 produced changes in beam attenuation (< 0.6%) and increases in skin dose (up to 55%) that were comparable to an unstretched Orfit head mask. During the experiments solid sections of the printing materials were used. In practice holes can be created within the masks to help to reduce skin dose. This can be further minimised by using as thin a material as possible, while still maintaining the rigidity of the shell. Compared to standard techniques it is not expected that the dosimetric changes introduced by these new materials will have a significant clinical impact on the treatment.

Initial pre-clinical trials of such shells will need to decide on the type of 3D printer and the material used. These decisions will depend on such factors as the 'build size' of the 3D printer, the size of the shell required, patient acceptability and cost. It is likely that 'negative' shells will be produced directly as printing 'positive' heads first seems unnecessary and it is significantly more expensive. Current soft drape masks cost approximately £30 - £65 depending on the size whilst printing just one shell using a commercial printer currently costs £80 (although mould room time is avoided). However, the printing costs are significantly reduced if multiple masks or other objects such as bolus can be printed within the same build chamber [13]. In the last five years we have seen the 3D printing and rapid prototyping industries really push the boundaries in technology and materials. Mid-range devices have become available at significantly cheaper prices bringing down the costs of printing and the authors believe that as the technology develops and the applications in medicine become more numerous that it will become viable for a large hospital or perhaps a cluster of smaller hospitals to have access to their own high end 3D printer for medical applications. Some 3D printing materials are already certified for use within surgical applications. In terms of time print jobs could be initiated at the end of the working day enabling the completed models to be extracted with limited post-processing the next morning.

It is of paramount importance that any radiotherapy shell employed using 3D printing technology must be at least as efficient (and hopefully even more efficient) than a standard soft drape or BDS shell produced in the standard way in terms of immobilising the patient. Studies have suggested that both soft drape and BDS radiotherapy shells produced in a standard way do allow a certain amount of movement and hence the recommendation to employ some method of checking patient position prior to commencing each treatment [1,2-4,10,14, 15,16]. Rotondo et al. present an approach to calculate errors between immobilisation techniques by determining displacement errors between co-registered data sets of patients undergoing different immobilisation techniques [15]. Recently Kang et al. have investigated accuracy in positioning and immobilisation for head and neck cancer treatment and determine translational intrafractional errors by six DoF registration of less than 2mm, although they did find that there was substantial motion during treatment in some cases [16]. Future work to that discussed in this paper will be to conduct immobilisation studies of the proposed 3D printed radiotherapy masks along similar lines to those used by Sanghera and colleagues [10]. Provided these are satisfactory an application

will be made for ethical approval to carry out a prospective clinical comparison with radiotherapy shells produced in the standard way with patient-related but also treatment-related endpoints.

Conclusions

Techniques have been shown which create 3D printed immobilisation shells produced from patient data using CT or MRI. The majority of the possible candidate 3D printing materials tested result in very similar attenuation of a therapeutic RT beam as the Orfit soft-drape masks currently in use in many UK radiotherapy centres. The thickness of the shell should obviously be kept to a minimum to prevent large increases in skin dose. In terms of imaging, it is clear that standard image acquisitions can be used. The prototype CT used was created using thicker slices than typically used for radiotherapy planning. The MRI sequence was created with 2 mm slices covering from the vertex of the skull to the upper shoulders which took less than 12 minutes. Image acquisition would in practice need to be in the intended treatment position according to the site to be irradiated.

In summary, 3D printed shells can be produced from CT and MRI datasets which will potentially avoid the moulding of shells directly to the patients' face. New shells could also be produced using the volumetric datasets acquired as part of an image-guided and adaptive radiotherapy programme. Associated cost is likely to be driven down by the emerging technology that is rapid prototyping.

Conflicts of Interest

None

REFERENCES

[1] Devereux C, Grundy G, Littman P. Plastic moulds for patient immobilisation. International Journal of Radiation Oncology Biology Physics 1976;1:553-557

[2] Gilbeau L, Octave-Prignot M, Loncol T, Ranard L, Gregoire V. Comparison of setup accuracy of three different thermoplastic masks for the treatment of brain and head and neck tumours. Radiotherapy and Oncology 2001;58:155-162

[3] Hess CF, Kortmann RD, Jany A, Hamberger M. Accuracy of field alignment in radiotherapy of head and neck cancer utilizing individualized face mask immobilisation: A retrospective analysis of clinical practice. Radiotherapy and Oncology 1995;34:69-72

[4] Schulte RW, Fargo RA, Meinass HJ, Slater JD, Slater JM. Analysis of head motion prior to and during proton beam therapy. International Journal of Radiation Oncology Biology Physics. 2000;47:1105-1110

[5] Sharp L, Lewin F, Johansson H, Payne D, Gerhardsson A, Rutqvist LE, Randomized trial on two types of thermoplastic masks for patient immobilization during radiation therapy for head and neck cancer, Int. J. Radiat Oncol Biol Phys, 2005; 61:250-256.

[6] Making a radiotherapy mask, Macmillan Cancer Support,

http://www.macmillan.org.uk/Cancerinformation/Cancertreatment/Treatmenttypes/Radiotherapy/Beforetreatment/Radiotherapymasks.aspx. Accessed 2014.

[7] Tam MD, Laycock S, Bell G D, Chojnowski A: 2012 3D printout of a DICOM to aid surgical planning in a 6year old patient with a large scapular osteochondroma complicating congenital diaphyseal aclasia. Radiological Case Jan;6(1):31-37

[8] Laycock, Bell GD, Mortimore D, Greco MK, Corps N, Finkle I. Combining X-ray Micro-CT technology and 3D printing for the digital preservation and study of a 19th Century Cantonese Chess piece with intricate internal structures. ACM Journal on Computing and Cultural Heritage, 5 (4). 13:1-13:7, 2013.

[9] Esses SJ, Berman P, Bloom AI, Sosna J. Clinical Applications of Physical 3D Models Derived from MDCT Data and Created by Rapid Prototyping. AJR 2011;196:W683-W688

[10] Sanghera B, Amis A, McGurk M. Preliminary study of the potential for rapid prototype and surfaced scanned radiotherapy facemask production technique. J. of Medical Eng. and Technology 2002;26:16-21

[11] McKernan B, Bydder S, Deans T, Nixon MA, Joseph DJ, Surface laser scanning to routinely produce casts for patient immobilization during radiotherapy, Australas Radiol. 2007 Apr;51(2):150-3.

[12] Hulse M, Isherwood S Scrase C, Laycock S, Bell GD. 3D CT-aided modelling of treatment shells for use in Radiotherapy. Presented at the National Cancer Research Institute (NCRI)Clinical and Translational Radiotherapy Research Working Group (CTRad) Clinical Trials Workshop, 27th February 2012, Leeds

[13] W Zou, T Fisher, B Swann, R Siderits, M McKenna, A Khan, N Yue and M Zhang, MO-H-19A-03: Patient Specific Bolus with 3D Printing Technology for Electron Radiotherapy, Med. Phys. 41, 443, 2014;

[14] Kim H, Park Y-K, Ki, IH, Ye S-J. Development of an optical-based image guidance system: Technique detecting external markers behind a full mask. Med. Phys. 2011;38:3006-3012

[15] Rotondo RL, Sultanem K, Lavoie I, Skelly J, Raymond L. Comparison of repositioning accuracy of two commercially available immobilization systems for treatment of head-and-neck tumors using simulation computed tomography imaging. Int J Radiat Oncol Biol Phys. 2008 Apr 1; 70(5):1389-96.

[16] KANG, Hyejoo et al. Accurate positioning for head and neck cancer patients using 2D and 3D image guidance. Journal of Applied Clinical Medical Physics, [S.l.], v. 12, n. 1, Oct. 2010. ISSN 15269914.